

A biological sub-micron thickness optical broadband reflector characterized using both light and microwaves

P Vukusic, R Kelly and I Hooper

J. R. Soc. Interface 2009 **6**, S193-S201 first published online 28 November 2008
doi: 10.1098/rsif.2008.0345.focus

References

This article cites 31 articles, 5 of which can be accessed free
http://rsif.royalsocietypublishing.org/content/6/Suppl_2/S193.full.html#ref-list-1

Article cited in:

http://rsif.royalsocietypublishing.org/content/6/Suppl_2/S193.full.html#related-urls

Subject collections

Articles on similar topics can be found in the following collections

[biomimetics](#) (8 articles)
[biophysics](#) (70 articles)
[nanotechnology](#) (19 articles)

Email alerting service

Receive free email alerts when new articles cite this article - sign up in the box at the top right-hand corner of the article or click [here](#)

To subscribe to *J. R. Soc. Interface* go to: <http://rsif.royalsocietypublishing.org/subscriptions>

A biological sub-micron thickness optical broadband reflector characterized using both light and microwaves

P. Vukusic*, R. Kelly and I. Hooper

School of Physics, University of Exeter, Exeter EX4 4QL, UK

Broadband optical reflectors generally function through coherent scattering from systems comprising one of three designs: overlapped; chirped; or chaotic multilayer reflectors. For each, the requirement to scatter a broad band of wavelengths is met through the presence of a variation in nanostructural periodicity running perpendicular to the systems' outer surfaces. Consequently, the requisite total thickness of the multilayer can often be in excess of 50 µm. Here, we report the discovery and the microwave-assisted characterization of a natural system that achieves excellent optical broadband reflectivity but that is less than 1 µm thick. This system, found on the wing scales of the butterfly *Argyrophorus argenteus*, comprises a distinctive variation in periodicity that runs parallel to the reflecting surface, rather than perpendicular to it. In this way, the requirement for an extensively thick system is removed.

Keywords: iridescence; multilayer interference; diffraction; butterfly; structural colour

1. INTRODUCTION

One of nature's predator avoidance strategies comprises crypsis brought about by broadband reflectance. It is commonly found in the scales of some fishes (Land 1972), in the elytra of some Coleoptera (Neville 1977; Parker *et al.* 1998), and in the cuticle of some lepidopteran pupae (Brink *et al.* 1995). The mechanism that generates such broadband reflection in documented cases invariably relies on coherent scattering from specific forms of multilayer reflector. In these, the incorporation of a distinct range of refractive index periodicities, rather than simply a single well-defined periodicity, establishes the requisite conditions for the reflection of a broad band of frequencies. The characteristic design of these systems usually falls into one of three distinct categories: overlapping systems in which separate individual multilayer reflectors (e.g. with stop bands at red, green and blue wavelengths) overlie each other (Land 1972); chirped multilayers (Neville 1977; Nishida *et al.* 2002) in which there is a gradual increase or decrease in refractive index periodicity with distance from the surface of the system; and chaotic reflectors (Denton & Land 1971; McKenzie *et al.* 1995) in which there is a randomly arranged spatial variation in the periodicity of the system's multilayer. In all three of these systems, the direction of periodicity variation is essentially perpendicular to the sample's (and each layer's) surface.

Generally with natural multilayer systems, the difference in refractive index between the two constituent

media is rather limited when compared with synthetic multilayer systems. It is approximately 0.3 for some Coleoptera, approximately 0.5 for fishes and approximately 0.6 for Lepidoptera (Land 1972), whereas for synthetic systems comprising, say, ZnS and MgF₂ multilayers, this refractive index difference is approximately 1.1. Accordingly in natural systems, large numbers of layers are usually required to produce high-intensity broadband reflectance (Land 1972). This therefore creates the requirement that, for a functionality involving bright mirror-like reflection, these natural broadband reflector systems must necessarily be very thick, sometimes much in excess of 50 µm (Steinbrecht *et al.* 1985). Biologically, this thickness appears to be an acceptable burden for many species since thick broadband reflectors are known to have evolved in many different animal phyla (Neville 1977), the single preferred design in each case determined by complex ecological, morphological and developmental pressures.

In Lepidoptera, wing colour is determined almost without exception by the scales that imbricate each wing surface (Nijhout 1991). They are already well recognized for their advanced photonic ultrastructural designs (Ghiradella 1991; Vukusic *et al.* 2000a,b; Ingram & Parker 2008). Despite their very limited thickness, a trait imposed by the design of the characteristic scale template, relatively minor elaborations of the common architectural elements present in this generic scale will produce the many forms responsible for structurally generated colour in Lepidoptera (Ghiradella 1984). Their thicknesses, however, are generally limited; the thickest scales reported so far are of the order of approximately 5 µm for a few individual species; however, a more typical thickness is between approximately 1 and 2 µm.

*Author for correspondence (p.vukusic@ex.ac.uk).

One contribution of 13 to a Theme Supplement 'Iridescence: more than meets the eye'.

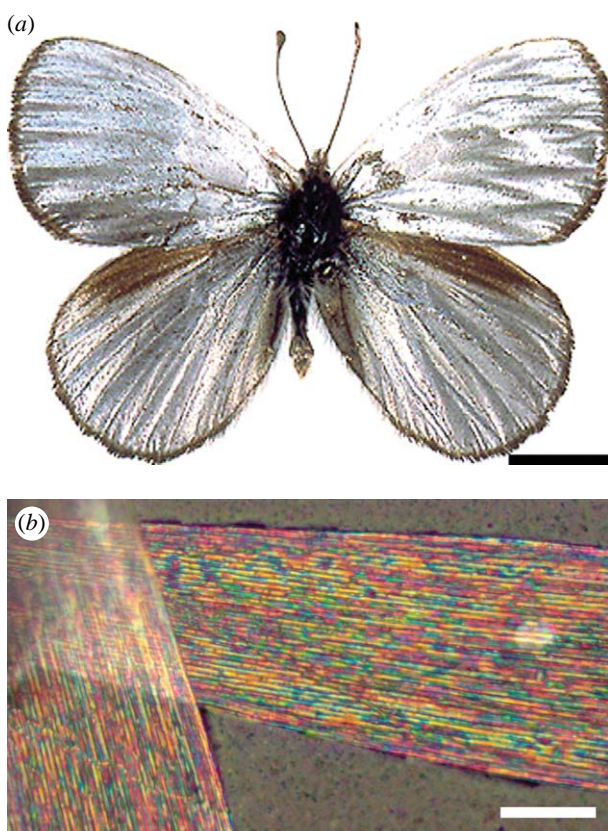


Figure 1. (a) Photograph of an *A. argenteus* specimen's dorsal wing surfaces, taken in diffuse white illumination. (b) Optical microscope epi-mode image of two single structurally coloured scales from the *A. argenteus* right forewing imaged in (a). Scale bars: (a) 0.5 cm and (b) 15 μ m.

While unsaturated structural colours in Lepidoptera are not uncommon, broadband reflection is rare. Several small area gold or silver coloured patches do adorn the wings of only a very limited set of Lepidoptera (Brink *et al.* 1995; Giraldo 2008). These patches and their associated optical signatures appear to form a very small component of the overall wing appearance of the species studied. The reason for such paucity may in part be attributed to the possible upper limit of thickness in lepidopteran wing scales: a thickness of no more than several micrometres is insufficient to accommodate effectively one of the three conventional forms of broadband multilayer reflector (Land 1972).

There appears to be only very few lepidopteran species from which there is broadband reflectivity from an especially large wing area. One of these is the butterfly *Argyrophorus argenteus* (Blanchard 1852) that is diffusely silver in appearance across the majority of both its dorsal (figure 1a) and ventral wing surfaces. It is a *Nymphalid* that is found between 1000 and 2200 m in the Andes on the border of Chile and Argentina. It appears to have overcome the design challenge associated with creating an efficient broadband reflection using very limited reflector thickness.

In this paper, we report the characterization of this butterfly's broadband reflecting system using microscopy, visible light spectroscopy and a novel

technique in which a scaled-up highly accurate replica of the scale structure is fabricated synthetically and interrogated with microwave radiation.

2. MATERIAL AND METHODS

2.1. Samples

The investigated *A. argenteus* specimens were all male butterflies, obtained from Worldwide Butterflies, UK.

2.2. Optical microscopy

Whole wing regions and carefully selected individual single scales were examined in reflection and transmission under bright and dark field polarized and unpolarized illumination, using a Carl Zeiss Axioskop 2 polarizing microscope (Imaging Associates, Cambridge, UK). Images were captured using a high-resolution AxioCam MRc5 digital camera. Single scales were optically imaged while positioned at specific known locations on the surface of a glass slide that had been patterned with a reference two-dimensional micro-grid using scanning electron microscopy (SEM) (FEI Nova) with a focused-ion beam ELPHY Quantum Lithography attachment (RAITH GmbH). This made it possible to locate and image the same individual specific scales using first optical and then electron microscopy.

2.3. Scanning and transmission electron microscopy

The butterfly wing regions and individual scales were investigated by SEM and transmission electron microscopy (TEM), using an Hitachi S-3200N SEM and a JEOL 100S TEM. Prior to SEM, the samples and substrates were sputtered with 5 nm of chromium (for 3 min at 1 kV and 150 mTorr) in a Cressington sputter coater (208 HR). Using substrates with the reference micro-grid described in §2.2, SEM images were taken of the same scales whose optical images had already been taken using the Axioskop optical microscope.

TEM images were taken after fixing samples in 3 per cent glutaraldehyde at 21°C for 2 hours followed by rinsing in sodium cacodylate buffer. Samples were then fixed in 1 per cent osmic acid in buffer for 1 hour followed by block staining in 2 per cent aqueous uranyl acetate for 1 hour, dehydration through an acetone series ending with 100 per cent acetone and embedding in Spurr resin. Post-microtomed sample sections were stained with lead citrate.

2.4. Spectrophotometry

Optical reflection data from the *A. argenteus* dorsal and ventral wing surfaces were recorded with an Ocean Optics DH-2000-BAL source as the illuminant. It was brought to a small diameter focus on the wing using an F1.5 achromat. The wavelength-dependent reflection was collected using an Ocean Optics UV-Vis 400 μ m diameter optical fibre connected to an Ocean Optics HR4000 high-resolution UV-Vis-IR spectrometer.

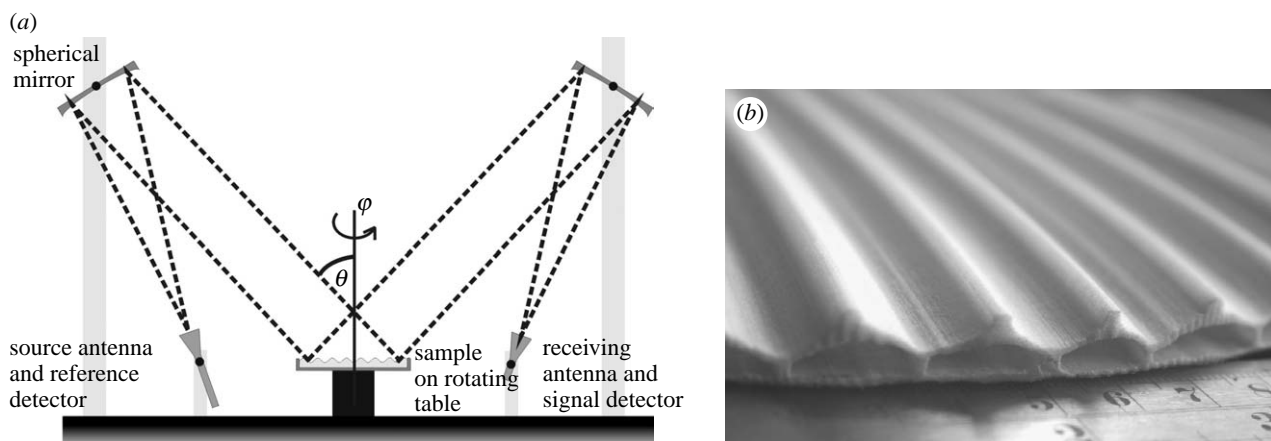


Figure 2. (a) Experimental arrangement for data collection using a microwave source and detector, and an approximately $\times 20\,000$ scaled-up sample (shown in (b)) fabricated by SLS with a cross section identical in form to an original *A. argenteus* scale cross section.

2.5. Microwave sample fabrication and characterization

TEM grey-scale images of the butterfly samples' silver scale cross sections were digitized and imported to RHINOCEROS NON-UNIFORM RATIONAL B-SPLINES software. These two-dimensional images were digitally extruded to form three-dimensional virtual models and dimensionally increased in size and in proportion by a factor of approximately 20 000 in relation to the original dimensions. These virtual models were then exported to selective laser sintering (SLS) equipment (DTM Sinter Station) and three-dimensional models were fabricated. SLS is an established industrial process in which a high-power laser selectively fuses powdered thermoplastic material by scanning successive cross sections of a three-dimensional computer model on to the smoothed surface of a powder bed of the material. After one cross section is written, the powder bed is lowered by one section thickness and the process repeated so that the full three-dimensional computer model may be built up layer by layer. Each powder layer thickness is $50 \pm 5 \mu\text{m}$. The prototyping material used for the fabrications in this investigation was Duraform polyamide (3D Systems Europe Ltd). The fabricated models represented accurate scaled-up versions based explicitly on the high-resolution TEM images of the *A. argenteus* scale structure. The scaling factor was selected so that the behaviour of the real butterfly structure at optical wavelengths would be duplicated at the gigahertz frequencies (microwave wavelengths) accessible in our laboratory environment.

Figure 2a illustrates the experimental arrangement used to record the reflectivity from the model sample (figure 2b). It is an arrangement that was developed to minimize the spherical nature of wavefronts emerging from the microwave horn source which would normally be associated with standard microwave source geometries (Hibbins & Sambles 2000). Whereas, normally, the beam divergence from such horn sources is in excess of 25° , by placing the transmitting horn at the focus of the 2 m focal length mirror indicated in figure 2a, the incident beam may be very well collimated and its associated beam divergence reduced

to approximately 1° . A second mirror, positioned to collect and focus the beam that is specularly reflected from the sample to the collecting horn, forms the detection facility. These two reflecting mirrors were milled with a diameter of 450 mm and a radius of curvature $R=4$ m from aluminium alloy. In this study, the reflectivity data are taken as a function of wavelength, polarization and both the angle of incidence (θ) and the sample's azimuthal angle (ϕ). The source and receiving horn antennas were set to pass either *p*-(TM) or *s*-(TE) polarizations. To account for any fluctuations in the emitted power from the source, the analyser that measures the reflected signal divides the output from the signal detector by that from the reference. The normalized reflectivities over the entire frequency range were downloaded from a scalar network analyser to a PC and saved to disk. The resulting wavelength-dependent reflectivities from the sample were normalized by comparison with the reflected signal from a flat metal plate (a near-perfect microwave mirror) of exactly the same dimensions.

2.6. Theoretical modelling

The dielectric response of the *A. argenteus* structures was modelled using two methods. The first was based on the Chandeson transformed coordinate approach that was extended for multilayer systems with interfaces that have common periodicity but arbitrary profile (Chandeson *et al.* 1982; Preist *et al.* 1995; Vukusic *et al.* 2000b). The usefulness of the Chandeson method is that it introduces a new coordinate framework for calculations involving Maxwell's equations on a structured system, transforming periodically modulated surfaces into planar surfaces and allowing straightforward matching of electromagnetic boundary conditions. Consequently, numerical modelling of the periodic structures becomes straightforward and it is perfectly adapted for modelling multilayer coated periodic structures or periodically modulated multilayers.

The model used for this method was relatively simple but nevertheless mimicked the general form of the structure's cross section for its interaction with

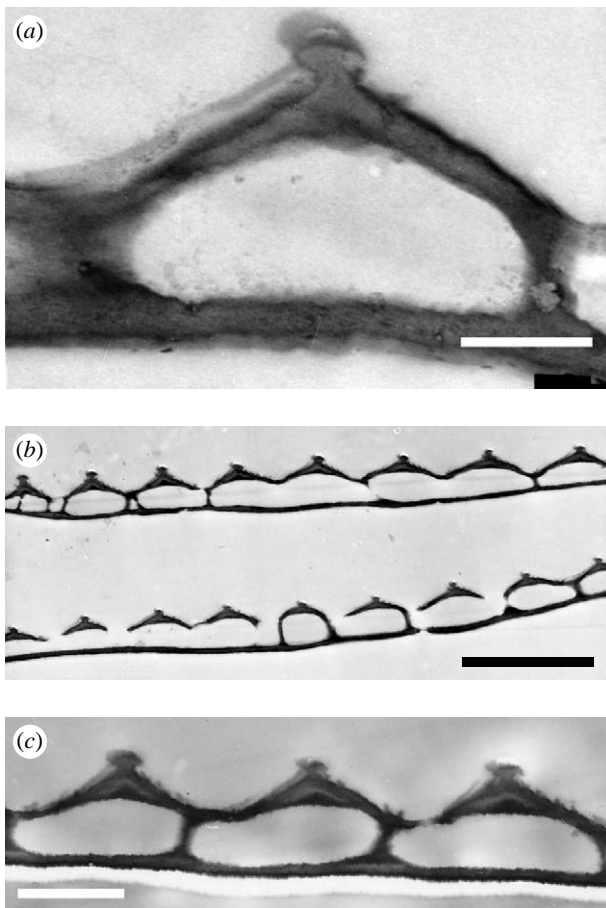


Figure 3. (a–c) Transmission electron micrographs of cross sections from *A. argenteus* structurally coloured wing scales. Scale bar: (a) 120 nm; (b) 3 μ m and (c) 400 nm.

microwave radiation. It comprised three semi-infinite layers: a flat basal layer of material of thickness 1.2 mm; an upper material layer with a sinusoidally varying profile of pitch 1.5 cm and thickness 1.2 mm; and an air gap between these two, the thickness of which varied between 5 and 7 mm. The refractive index (at this microwave frequency range) of the thermoplastic constituent material was determined to be 1.51 using established techniques (Sambles *et al.* 2006) and was used for the modelling.

The second modelling method was the finite-element method (FEM) (Ansoft HFSS, www.ansoft.com). The structure representing a characteristic unit cell from an *A. argenteus* scale (i.e. its repeating cross-sectional profile) was created digitally using mean dimensions that were measured from TEM images (figure 3). The material was assigned a refractive index $n=1.56$ (Land 1972; Vukusic *et al.* 1999) for optical band modelling. The optical absorption that is usually associated with the presence of broadly optically absorbing pigment in the scale was assumed to be negligible (this is evident from the region of overlapping scales in figure 1b and was set to zero in the model). Additionally, to understand and verify the experimental response of the scaled-up SLS-fabricated replica, an equivalently scaled-up (approximately $\times 20\,000$) digital model was created to investigate its electromagnetic response at microwave frequencies.

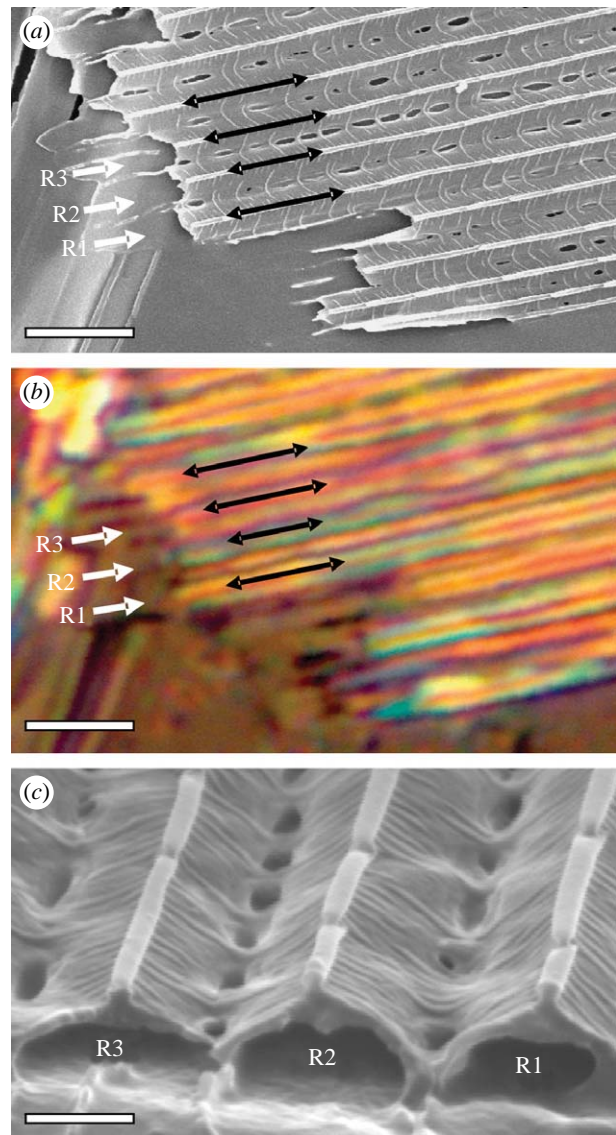


Figure 4. (a, b) SEM and optical microscope images, respectively, of an identical intra-scale region forming part of one structurally coloured *A. argenteus* scale, taken from directly above the sample. Four corresponding ridge lines of these two images are indicated by the black arrows: three open-ended ridge structure regions are indicated by the white arrows and labels R1, R2 and R3. These open-ended structures are then indicated and shown by the image in (c) that was taken from near grazing angle. Scale bar: (a, b) 3 μ m and (c) 0.8 μ m.

3. RESULTS

Under optical microscopy individual multiply coloured strips are clearly observed running the full length of each *A. argenteus* wing scale (figures 1b and 4b). Macroscopically, when the juxtaposed strips can no longer be individually resolved, they additively combine to synthesize the stimulus (Burnham *et al.* 1963) of broadband silver colour.

Direct comparison between optical images and SEM images of the same individual intra-scale regions (figure 4a, b), indicate that individual strips of colours correspond to specific regions within the cross-sectional profile of the scale structure. Also, close comparison of these images shows that nominal variations in the

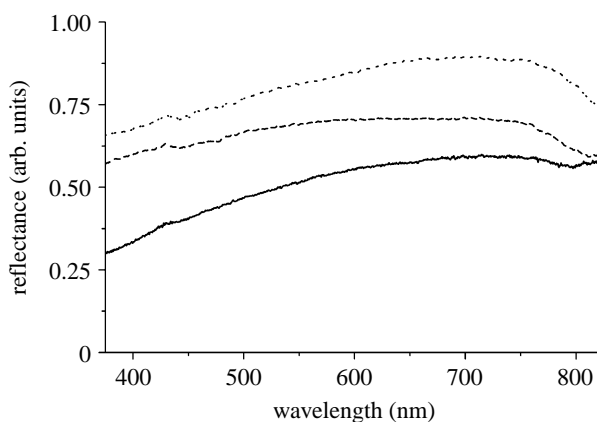


Figure 5. Optical reflectivity data taken from the dorsal wing surface of *A. argenteus* (solid line). The reflectivity data from the dull and polished surfaces (dashed line and dotted line, respectively) of household aluminium foil, taken under identical conditions, is presented for comparison.

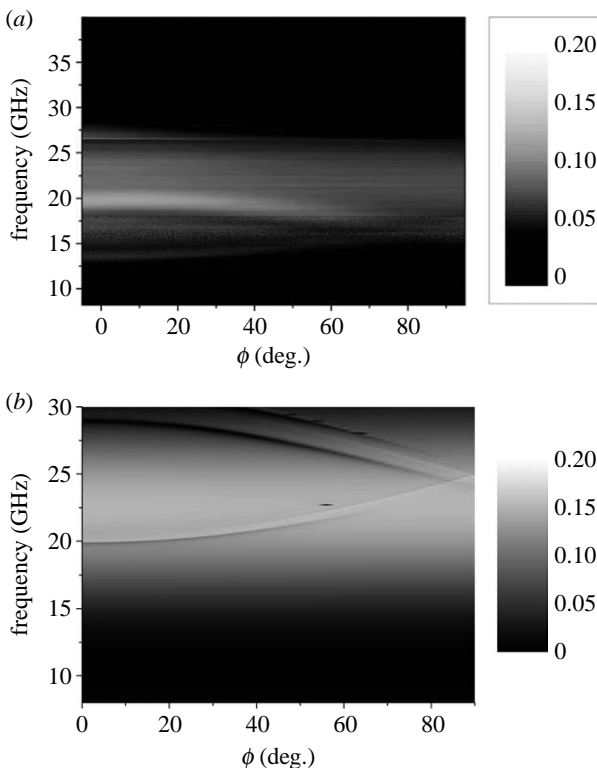


Figure 6. (a) Microwave experimental TM-polarized reflectivity data (reflected intensity as a function of incident frequency and sample azimuthal angle) taken from the SLS-fabricated sample. (b) TM-polarized theoretical data (also reflected intensity as a function of incident frequency and sample azimuthal angle) generated using a very simplified model of the sample structure.

nature of the scales' minor surface features, such as scale ridge spacing, the presence or absence of microribs and any porosity of the surface layer, do not notably affect the colour banding at the resolution of the light microscope.

Figure 5 shows the typical optical reflectance spectrum from the dorsal forewing surface of *A. argenteus*. This reflection is very similar to that from both the dull and the polished surfaces of household

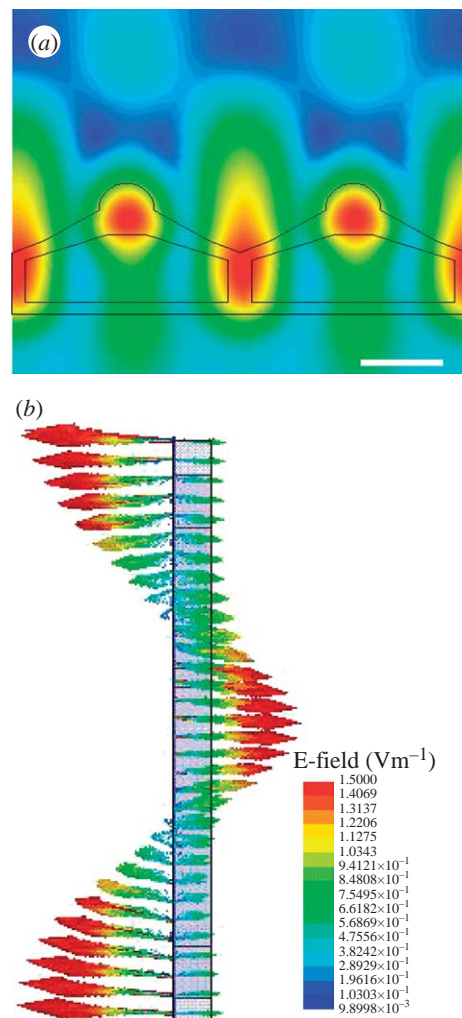


Figure 7. *E*-field magnitude plotted (a) in the *xz*-plane (showing two neighbouring unit cells; scale bar: 500 nm) and (b) in the *xy*-plane (i.e. viewed from above one unit cell) of the optical scale model at a temporal phase corresponding to maximum local field enhancement under normally incident 500 nm wavelength light at azimuthal angle $\phi = 0^\circ$.

aluminium foil, which were recorded for comparison. The broad band of the reflectivity from the wing surface extends beyond the optical range, from approximately 350 nm to 1.3 μ m, although scattering from the wing substrate underneath the scales becomes more dominant beyond the limit of approximately 1.1 μ m.

Reflectivity measured from the microwave scale sample, using the gigahertz frequency interrogation technique described earlier, is presented in figure 6a (this is one representative set of data recorded at an 8° angle of incidence using a TM polarized source). It shows the selective reflection of a broad band of frequencies between approximately 13 and 28 GHz. There is some fine structure within this reflected band that is highly dependent on the azimuthal angle. This broad band and the fine structures within it correspond well to the results of the Chandezon modelling method applied to the relatively simple model (figure 6b). Figure 7a,b represents results from the FEM optical modelling. Two neighbouring unit cells (which represent typical neighbouring unit cells based on that which is shown in the TEM of figure 3a) are shown in

cross section by the black lines in **figure 7a**. In **figure 7b** one unit cell segment is shown directly from above. The regions of *E*-field maxima are represented by the red coloured regions in **figure 7a** and the red coloured arrows in **figure 7b**. They show the instantaneous *E*-field magnitude plotted in the *xz*-plane in **figure 7a** and the instantaneous *E*-field vectors plotted in the *xy*-plane across the unit cell of the optical scale model at a temporal phase corresponding to maximum local field enhancement and at incident wavelength of 500 nm. This modelling and these field plots imply that, in addition to the broad band of reflection shown in **figure 6a** (experimental results) and **figure 6b** (theoretical modelling), the incident electromagnetic fields undergo very strong resonances with the intra-scale structure. **Figure 7** indicates that *E*-field maxima are localized around the structures that are periodic within the scale's unit cell (i.e. the scale's ridges and the cuticular walls that signify the horizontal boundary of each unit cell). This is indicative of a resonance coupling phenomenon. In this case, it is due to the diffractive scattering associated with these periodic structures, on and in the scale, which enables light coupling to optical guided modes which propagate through the system (Saleh & Teich 1991). The direction of this propagation, contrary to intuition, is perpendicular to the scales' ridging.

4. DISCUSSION

Individual wing scales from across *A. argenteus* butterflies' dorsal and ventral surfaces present identical optical characteristics. At the microscopic scale they exhibit narrow multiply coloured strips that run parallel to each scale's long axis (**figures 1b** and **4a**). It is the quasi-random variation in colour between these neighbouring bands and along each band's length, concurrent with their close juxtaposition, which creates the overall broadband silver appearance of the butterfly's wings. The effect of additive colour mixing, sometimes called colour stimulus synthesis (CSS), found in some beetles (Schultz & Bernard 1990) is already documented in some Lepidoptera that combine yellow and blue juxtaposed colour centres for the creation of a green coloured appearance (Vukusic *et al.* 2000b, 2001). However, lepidopteran use of CSS to create broadband silver coloration by using a broader colour range of juxtaposed neighbouring coloured regions, as described here for *A. argenteus*, does not yet appear to have been documented. A different mechanism, comprising chirped multilayer systems, is responsible for the broadband silver appearance of some iridescent lepidopteran pupae (Steinbrecht *et al.* 1985).

The designs of all lepidopteran scales, pigmentarily coloured, structurally coloured or otherwise, are understood to be based on an ancestral generic scale template design (Ghiradella 1984, 1985). This design is principally dominated by the way in which each scale is formed. Scales are extruded from a single epidermal cell: a growing scale cell lays down a thin plastic outer layer of cuticle, first around itself as the secretion and assembly of cuticle takes place extracellularly, then on the structures within (Ghiradella 1984, 1994, 1998).

When the cell finally dies back into the epithelium of the wing, the newly formed scale dries and hardens to leave the finished functional product (Ghiradella 1998). This comprises near-parallel ridges that run the scale's length and which are interconnected by ribbed structures which themselves form a layer or rest on a membrane that is the upper layer of the scale. This layer is spatially separated from a basal layer by a gap that is usually largely air filled. In some cases, the ridges or the upper or basal layers, or internal volume, may be highly customized with nanostructure that is periodic in one, two or three dimensions (Vukusic *et al.* 2000a,b). In *Morpho*-type structures, the ridges themselves are adapted to form spatially discrete multilayers (Vukusic *et al.* 1999; Yoshioka & Kinoshita 2003; Berthier *et al.* 2006). In *Urania* and some *Papilio* species (Huxley 1976; Ghiradella 1985; Vukusic *et al.* 2001; Yoshioka & Kinoshita 2007), the ridging ceases to play a significant optical role; however, the scale's dorsal layer itself is elaborated into a continuous multilayer which may be flat or locally curved. In other lepidopteran species, such as *Parides sesostris*, *Teinopalpus imperialis* and *Cyanophrys rubi*, the volume between the dorsal and basal layer is occupied by a three-dimensional periodic network of cuticle (Allyn & Downey 1976; Ghiradella 1994; Vukusic & Sambles 2003; Prum *et al.* 2006; Michielsen & Stavenga 2008). In limited other examples, namely one family of Afrotropical *Papilio*s, a scale design has evolved in which the dorsal layer is elaborated into a two-dimensional photonic crystal slab infused with fluorescent pigment while the basal layer, spatially separated from the dorsal layer by about 1 µm, is itself formed of a multilayer (Huxley 1976; Vukusic & Hooper 2005).

For the *A. argenteus* wing scales studied here, the scale design and ultrastructural origin of their coloured banding are revealed by TEM and SEM (**figures 3** and **4**). The generic scale template design appears modified relatively simply. Each *A. argenteus* wing scale comprises two outer cuticular layers, one dorsally and one basally situated. These are separated by an air gap containing longitudinal partitions that create corridor-like configurations (**figure 4c**). The basal layer is perfectly continuous and approximately 120 nm thick. The dorsal layer is also continuous except for small (no more than 2–3 µm diameter) irregularly spaced pores. It connects neighbouring ridges throughout the scale surface in such a way that its thickness varies from approximately 200–250 nm in the region of each ridge to approximately 100 nm in the region between ridges. The dorsal layer surface profile is of a form approximating a small amplitude symmetric sawtooth (**figure 3** inset). This profile imposes a concurrent variation in the thickness of the air gap between the dorsal and ventral layers. It is a structural design that not only coherently scatters visible light to produce colour but it simultaneously presents a range of periodicities that run parallel to the scale surface. It is this range that results in the scatter of a broad band of wavelengths and the production of its macroscopic silver hue through additive colour mixing.

Figure 4a,b compares the same single intra-scale region, imaged temporally first by optical microscopy

and then by SEM. The SEM image in figure 4c shows the intentionally exposed cross section of a three-ridge region (labelled R1, R2 and R3) within the area shown in figure 4a,b. The direct effect of the variation in dorsal layer and air gap thickness is revealed by comparing the colour banding pattern in figure 4a with the exposed layer thicknesses in the identical region in figure 4b. The intra-scale bands of the same colour run in the direction parallel to the ridges for distances of between one or two micrometres and tens of micrometres. The hue variations in this direction are brought about by gradual changes in cuticle layer and air gap thicknesses after specific distances in the direction that is parallel to the ridge structures.

Despite the use of an established single scale characterization technique (Vukusic *et al.* 1999), full and complete characterization of the scale structure's interaction with incident light was not accessible. For this reason, accurate scaled-up models of the intra-scale region of a typical scale were fabricated using SLS (see §2). These models were interrogated using a microwave wavelength band that was approximately 20 000 times longer than that of visible light, using the method described earlier. By investigating the dependence of the reflectivity from this model with incident polarization, incident angle and sample azimuthal angle (ϕ), in conjunction with the optical wavelength characterization of the real butterfly sample, a more complete understanding of the *A. argenteus* scale structure's interaction with appropriate incident radiation becomes accessible.

The microwave experimental data in figure 6a show two key features, one of which was not possible to detect using optical characterization only. The first feature is the broad band of reflection that is discernible between approximately 13 and 28 GHz. This is equivalent to the band of optical reflectivity (figure 5) that macroscopically makes each real wing scale silver in optical appearance. The second feature is the presence of resonant guided modes in the system. These are represented in the data by the distinctly curved bright and dark lines within the reflection band. They correspond to strong resonances associated with incident light that is diffractively coupled to the structure via scattering from the periodicity associated with the ridging direction (i.e. they disappear when the plane of incidence is parallel to the ridging at $\phi=90^\circ$). Though certainly present in the reflection characteristics of real *A. argenteus* butterfly scales, they are not discernable using currently available methods of optical characterization. The nature of these resonances and the structure's electromagnetic response were modelled in two different ways. The first using modelling based on Chandeson's transformed coordinate method described earlier. The theoretical data from this model are presented in figure 6b for direct comparison with the experimental data in figure 6a. Despite using the simplified model, both theory and data share the same essential features, namely a single broad band of brightly reflected frequencies that comprises distinct resonantly coupled guided modes. The difference in guided mode positions between theory and experiment is due to the relative simplicity of the model used compared with the real scale structure.

Using the second modelling technique, the FEM, a unit cell structure representing a single scale's characteristic repeating cross-sectional profile, was created (two of these, neighbouring each other, are shown in figure 7a). At optical wavelengths the electric fields associated with the resonantly coupled modes observed in the system were investigated. Strong electric field maxima appear centred around the scale ridges and the cuticular walls that partition the central air gap (figure 7a,b shows these electric field profiles for the guided mode reflectivity minimum condition at 500 nm and at azimuthal angle $\phi=0^\circ$). These fields occur extremely strongly in this configuration due to the electromagnetic boundary conditions that are imposed on the system by the cuticular structures. These *E*-fields, shown by the colour scheme in figure 7, represent the fundamental electromagnetic interaction between incident light and the butterfly's structure that is responsible for the resonant modes present in the experimental and theoretical data shown in figure 6. They are rather more pronounced in the theoretical modelling of figure 6b than in the experimental results of figure 6a because the modelling is based on the ideal structure of an infinite series of co-joined identical unit cells. The experimental microwave-scale replica is conversely based on the actual TEM cross section taken from an *A. argenteus* wing scale. Owing to this, therefore, and the inherent variation in the structural dimensions for each neighbouring cell and ridge spacing, the coupling is less efficient and the resonances observed in the experimental data are less clearly defined. Further investigation is underway to assess whether these modes may offer any real functionality.

The advantage offered by the design of this scale system over the three other recognized broadband reflector designs in natural systems is in relation to thickness. In examples such as beetle exocuticle (Neville 1977), copepods (Nishida *et al.* 2002) and fishes (Denton & Land 1971), there appears to be no obvious morphological requirement for their reflecting systems to be less than 2 μm thick. For this reason, the broadband reflector designs they have evolved can often be in excess of 50 μm thick (Steinbrecht *et al.* 1985). These very thick systems, incorporating an extremely large number of layers, offer the advantage of higher reflectivities (Land 1972). The lepidopteran scale template, however, on which the design of the *A. argenteus* reflecting system appears to be based, does place a several micrometre limit on overall thickness. The *A. argenteus* scale structure is an elegant way to cope with this limitation while still producing an effective broadband reflector. In doing so, it has evolved a very effective silver appearance using an extremely thin reflecting system. It does this by creating a lateral range of periodicities within the vertical periodicity that forms its multilayer.

Owing to the nature of the scale imbrication, the unevenness of the scale surfaces, and also the colour mixing effect, the broadband silver reflection from this wing appears remarkably diffuse rather than specular. This may offer an advantage for mirror crypsis since it further reduces the conspicuousness that may be associated with the flash nature of specular reflectivity.

The accuracy of the large-scale three-dimensional replica may be improved further. For the models used in this investigation, single TEM images of scale structure cross sections (taken in the xz -plane shown in figure 3) were extruded in the y -direction. This prevents incorporation into the model of any structural variation in the y -direction itself. We are working to overcome this limitation by appropriately combining the digitized images of consecutively microtomed 50 nm thick sections. By suitably ordering, aligning and interpolating between the two-dimensional profiles of these sections in the y -direction, more realistic models may be created digitally and subsequently fabricated and investigated. This is the subject of further work for the *A. argenteus* system described here and also for other animal systems.

5. CONCLUSION

The *A. argenteus* wing-scale structure has been characterized using electron microscopy and both optical and microwave interrogation methods. Its unusual colour appearance arises from a sub-micron thickness scale design that creates broadband diffuse silver reflectivity by multi-colour addition. This is achieved by incorporation of a unique design variation into its constituent multilayer reflector, one in which the required range of periodicities lies in the direction that is parallel to the surface rather than perpendicular to it as is the case with the much more common forms of natural broadband reflectors. Biomimetically, this *A. argenteus* scale design offers the basis for ultra-thin synthetic broadband reflectors, across a range of wavelength bands not limited only to visible wavelengths.

The microwave interrogation method described here and applied to this investigation is introduced as a method that may usefully complement the conventionally used all-optical techniques for characterizing such systems. It is especially appropriate for those natural samples, the geometries and physical sizes of which render them difficult to manipulate physically and analyse optically.

REFERENCES

Allyn, A. C. & Downey, J. C. 1976 Diffraction structures in the wing scales of *Callophrys (Mitoura) siva siva* (Lycaenidae). *Bull. Allyn Mus.* **40**, 1–6.

Berthier, S., Charron, E. & Boulenguez, J. 2006 Morphological structure and optical properties of the wings of Morphidae. *Insect Sci.* **13**, 145–158. (doi:10.1111/j.1744-7917.2006.00077.x)

Brink, D. J., Smit, J. E., Lee, M. E. & Möller, A. 1995 Optical diffraction by the microstructure of the wing of a moth. *Appl. Opt.* **34**, 6049–6057. (doi:10.1364/AO.34.006049)

Burnham, R. W., Hanes, R. M. & Bartleson, C. J. 1963 *Color*. New York, NY: Wiley.

Chandezon, J., Dupuis, M. T., Cornet, G. & Maystre, D. 1982 Multicoated gratings: a differential formalism applicable in the entire optical region. *J. Opt. Soc. Am.* **72**, 839–846. (doi:10.1364/JOSA.72.000839)

Denton, E. J. & Land, M. F. 1971 Mechanisms of reflexion in silvery layers of fish and cephalopods. *Proc. R. Soc. Lond. A* **178**, 43–61. (doi:10.1098/rspb.1971.0051)

Ghiradella, H. 1984 Structure of iridescent lepidopteran scales: variation on several themes. *Ann. Entomol. Soc. Am.* **77**, 637–645.

Ghiradella, H. 1985 Structure and development of iridescent lepidopteran scales: the Papilionidae as a showcase family. *Ann. Entomol. Soc. Am.* **78**, 252–264.

Ghiradella, H. 1991 Light and colour on the wing: structural colours in butterflies and moths. *Appl. Opt.* **30**, 3492–3500.

Ghiradella, H. 1994 Structure of butterfly scales: patterning in an insect cuticle. *Microsc. Res. Tech.* **27**, 429–438. (doi:10.1002/jemt.1070270509)

Ghiradella, H. 1998 Hair, bristles and scales. In *Microscopic anatomy of invertebrates*, vol. 11A (ed. M. Locke), pp. 257–287. New York, NY: Wiley-Liss.

Giraldo M. A. 2008, Butterfly wing scales: pigmentation and structural properties. PhD thesis, University of Groningen, The Netherlands.

Hibbins, A. P. & Sambles, J. R. 2000 Coupling of near-grazing microwave photons to surface plasmon polaritons via a dielectric grating. *Phys. Rev. E* **61**, 5900–5906. (doi:10.1103/PhysRevE.61.5900)

Huxley, J. 1976 The coloration of *Papilio zalmoxis* and *P. antimachus* and the discovery of Tyndall blue in butterflies. *Proc. R. Soc. Lond. B* **193**, 441–453. (doi:10.1098/rspb.1976.0056)

Ingram, A. L. & Parker, A. R. 2008 A review of the diversity and evolution of photonic structures in butterflies, incorporating the work of John Huxley (the natural history museum, London from 1961 to 1990). *Phil. Trans. R. Soc. Lond. B* **363**, 2465–2480. (doi:10.1098/rstb.2007.2258)

Land, M. F. 1972 The physics and biology of animal reflectors. *Prog. Biophys. Mol. Biol.* **24**, 75–106. (doi:10.1016/0079-6107(72)90004-1)

McKenzie, D. R., Yin, Y. & McFall, W. D. 1995 Silvery fish skin as an example of a chaotic reflector. *Proc. B. Soc. Lond. A* **451**, 579–584. (doi:10.1098/rspa.1995.0144)

Michielsen, K. & Stavenga, D. G. 2008 Gyroid cuticular structures in butterfly wing scales: biological photonic crystals. *J. R. Soc. Interface* **5**, 85–94. (doi:10.1098/rsif.2007.1065)

Neville, A. C. 1977 Metallic gold and silver colours in some insect cuticles. *J. Insect Physiol.* **23**, 1267–1274. (doi:10.1016/0022-1910(77)90069-5)

Nijhout, H. F. 1991 *The development and evolution of butterfly wing patterns*. Washington, DC: Smithsonian Institution Press.

Nishida, S., Ohtsuka, S. & Parker, A. R. 2002 Functional morphology and food habits of deep-sea copepods of the genus *Cephalophanes* (Calanoida: Phaenidae): perception of bioluminescence as a strategy for food detection. *Mar. Ecol. Prog. Ser.* **227**, 157–171. (doi:10.3354/meps227157)

Parker, A. R., McKenzie, D. R. & Large, M. C. J. 1998 Multilayer reflectors in animals using green and gold beetles as contrasting examples. *J. Exp. Biol.* **201**, 1307–1313.

Preist, T. W., Cotter, N. P. K. & Sambles, J. R. 1995 Periodic multilayer gratings of arbitrary shape. *J. Opt. Soc. Am. A* **12**, 1740–1748. (doi:10.1364/JOSAA.12.001740)

Prum, R. O., Quinn, T. & Torres, R. H. 2006 Anatomically diverse butterfly scales all produce structural colours by coherent scattering. *J. Exp. Biol.* **209**, 748–765. (doi:10.1242/jeb.02051)

Saleh, B. E. A. & Teich, M. C. 1991 *Fundamentals of photonics*. New York, NY: Wiley.

Sambles, J. R., Kelly, R. & Yang, F. Z. 2006 Metal slits and liquid crystals at microwave frequencies. *Phil. Trans. R. Soc. A* **364**, 2733–2746. (doi:10.1098/rsta.2006.1850)

Schultz, T. D. & Bernard, G. 1990 Pointillistic mixing of interference colors in cryptic tiger beetles. *Nature* **337**, 72–73. (doi:10.1038/337072a0)

Steinbrecht, R. A., Mohren, W., Pulker, H. K. & Schneider, D. 1985 Cuticular interference reflectors in the golden pupae of *Danaine* butterflies. *Proc. R. Soc. Lond. B* **226**, 367–390. (doi:10.1098/rspb.1985.0100)

Vukusic, P. & Hooper, I. 2005 Directionally controlled fluorescence emission in butterflies. *Science* **310**, 1151. (doi:10.1126/science.1116612)

Vukusic, P. & Sambles, J. R. 2003 Photonic structures in biology. *Nature* **424**, 852–855. (doi:10.1038/nature01941)

Vukusic, P., Sambles, J. R., Lawrence, C. R. & Wootton, R. J. 1999 Quantified interference and diffraction in single *Morpho* butterfly scales. *Proc. R. Soc. B* **266**, 1403–1411. (doi:10.1098/rspb.1999.0794)

Vukusic, P., Sambles, J. R. & Ghiradella, H. 2000a Optical classification of microstructure in butterfly wing scales. *Photonics Sci. News* **6**, 61–66.

Vukusic, P., Sambles, J. R. & Lawrence, C. R. 2000b Structural colour: colour mixing in the wing scales of a butterfly. *Nature* **404**, 457. (doi:10.1038/35006561)

Vukusic, P., Sambles, J. R., Lawrence, C. R. & Wakely, G. 2001 Sculpted-multilayer optical effects in two species of *Papilio* butterfly. *Appl. Opt.* **40**, 1116–1125. (doi:10.1364/AO.40.001116)

Yoshioka, S. & Kinoshita, S. 2003 Wavelength-selective and anisotropic light-diffusing scale on the wing of the *Morpho* butterfly. *Proc. R. Soc. B* **271**, 581–587. (doi:10.1098/rspb.2003.2618)

Yoshioka, S. & Kinoshita, S. 2007 Polarization-sensitive color mixing in the wing of the Madagascan sunset moth. *Opt. Exp.* **15**, 2691–2701. (doi:10.1364/OE.15.002691)